Two- and Three-Body Kinematical Correlation in the Dissociative Recombination of H_3^+

D. Strasser,[1] L. Lammich,[2] S. Krohn,[1] M. Lange,[2] H. Kreckel,[2] J. Levin,[2] D. Schwalm,[2] Z. Vager,[1]
R. Wester,[2] A. Wolf,[2] and D. Zajfman[1,*]

[1]*Department of Particle Physics, Weizmann Institute of Science, Rehovot, 76100, Israel*
[2]*Max-Planck-Institut für Kernphysik and Physikalisches Institut der Universität Heidelberg, D-69029 Heidelberg, Germany*
(Received 10 July 2000)

Fragmentation patterns for dissociative recombination of the triatomic hydrogen molecular ion H_3^+ in the vibrational ground state have been measured using the storage ring technique and molecular fragment imaging. A broad distribution of vibrational states in the H_2 fragment after two-body dissociation and a large predominance of nearly linear momentum geometries after three-body dissociation are found. The fragmentation results are directly contrasted with Coulomb explosion imaging data on the initial H_3^+ geometry, compared to existing wave-packet calculations, and considered in the light of a simple physical picture.

DOI: 10.1103/PhysRevLett.86.779 PACS numbers: 34.80.Lx

From its conceptual simplicity the triatomic hydrogen molecule (H_3 and isotopomers) occupies a special place in molecular physics and quantum chemistry, in particular with regard to studies of nuclear motion on molecular potential surfaces. Indeed, the unbound electronic ground-state potential of H_3 was probed by several scattering experiments [1] and recently by predissociation of laser-populated H_3 Rydberg states [2–4]. Particular interest in the nuclear dynamics on the H_3 ground-state potential surface stems also from the dissociative recombination (DR) of the H_3^+ ion. This ion acts as a key species in the chemistry of the interstellar medium [5], and notably its abundance in diffuse interstellar clouds, strongly affected by the dissociative recombination with low-energy electrons, is still a matter of vivid discussion [6,7]. In the present work, using molecular fragment imaging techniques at a heavy-ion storage ring [8], we have obtained detailed information about the dissociative recombination of H_3^+ with respect to the internal excitation of the outgoing molecular fragments and to the kinematic correlations between the atomic products.

DR of internally cold H_3^+ ions with low-energy electrons can proceed only via two channels:

$$H_3^+ + e^- \rightarrow \begin{cases} H(1s) + H(1s) + H(1s) & \text{(1a)} \\ \text{or} \\ H_2(v) + H(1s)\,, & \text{(1b)} \end{cases}$$

where v denotes the vibrational quantum number of the outgoing molecular hydrogen fragment. By mechanisms still unexplained in detail, involving an interplay of electronic and nuclear motion, the initial electronic continuum state couples to the dissociative ground configuration of H_3 and the H atoms rearrange by three-body [Eq. (1a)] or two-body dissociation [Eq. (1b)], associated with a total kinetic energy release E_k of 4.76 eV for the three-body channel and of 9.23 eV for the two-body channel yielding $H_2(v = 0, J = 0)$, assuming zero relative energy of the electrons and neglecting any H_3^+ internal excitation.

Good control over the internal excitation of the H_3^+ ions is of particular importance in experiments on DR. At present this can be achieved efficiently by using fast (MeV) molecular ion beams in heavy-ion storage rings [6]. Yet, results from different experimental approaches still leave an uncertainty [9,10] of about a factor of 10 for the H_3^+ DR rate coefficient; moreover, theoretical results for the rate coefficient lie below the experimental findings by at least a factor of 100 [11] and also cannot reproduce the branching ratio between three- and two-body events, measured [12] to be about 3:1 at low electron energy using the heavy-ion storage ring technique. The detailed comparison between experiment and theory may still be affected by unexplored experimental perturbations; among other items such as external fields [9], a possible initial rotational excitation of the H_3^+ ions also introduces such uncertainties.

Our experiment was carried out at the test storage ring (TSR) located at the Max-Planck Institut für Kernphysik, Heidelberg, Germany [13]. H_3^+ ions were produced in an electron-impact ion source, brought to an energy of 1.431 MeV using a radio frequency quadrupole accelerator, and injected into the storage ring. The circulating beam of about 10^6 ions was kept stored up to $\sim$10 s. It was continuously merged with a 3.5 cm diameter, quasimonochromatic electron beam of the same average velocity over a length of 1.5 m, providing electrons at a typical density of 3×10^6 cm^{-3} with a transversal temperature of 6 meV and a longitudinal temperature of $\sim$0.1 meV in the comoving reference frame. Through electron cooling, this yielded an ion beam of low momentum spread and a diameter of only $\sim$0.8 mm after a cooling time of $<$3 s. The vibrational excitation in the stored H_3^+ ion beam was probed as a function of the storage time in a separate experiment, using Coulomb explosion imaging (CEI) [14,15]. Here, ions extracted from the ring are stripped in an ultrathin foil and the distances between the three H^+ fragments after a drift of a few meters reflect the initial nuclear coordinates in the H_3^+ ion; the method is sensitive to the probability density of the nuclear wave function and hence probes the

vibrational (but generally not the rotational) excitation. For H_3^+ in the TSR, all vibrationally excited states were found to have decayed after 2 s. However, the rotational excitation is expected to be substantial in the ion source and not to relax significantly during the storage time in the ring; indeed, the recombination results presented below suggest a considerable rotational excitation of the H_3^+ ions. Data taking of the events discussed below started at 3 s after injection.

Dissociative recombination of H_3^+ ions occurs in the electron-ion interaction region at near-zero relative energies corresponding to the 6 meV transversal electron temperature. The fragments from each recombination reaction move towards an imaging detector [16] located 6 m downstream, which event by event yields the number of fragments and their impact positions (and hence their transverse momenta). The kinetic energy release of the reaction leads to fragment distances up to ~33 mm, while the barycenters of the impact positions (corresponding to the conserved total transverse momentum of the reaction) lie within a spot of ~1 mm diameter for an event where all fragments are detected.

The high resolution of the transverse imaging (~0.1 mm), together with the sharp definition of the center of mass motion and the initial electronic energy, allows us to extract considerable detail on the kinematics of the H_3^+ recombination reaction even from the transverse projections alone. Two- and three-body recombination events, respectively, are uniquely identified by requiring their center of mass to lie within the central spot. Out of all events in which only two fragments are observed within the coincidence window (~300 ns), this cut retains ~17% as originating from the H + H_2 recombination channel, while it rejects the background from dissociative excitation in residual gas collisions as well as such three-body recombination events where (at an estimated single-hit efficiency of the detector of ~0.6) one of the fragments remained undetected. From the events with three observed fragments, ~70% were retained as true 3-H recombination after the cut.

For the two-body recombination channel, the distribution of the transverse fragment distance D on the imaging detector reveals the energy release of the reaction, which in turn carries information on the excitation of the H_2 fragments. The observed distribution $P(D)$ is shown in Fig. 1(a). As in earlier experiments [16] on diatomic-ion recombination, the distribution in D for a given energy release E_k has a characteristic shape [see dashed lines in Fig. 1(a)] resulting from the average over the dissociation angles and the longitudinal extent of the interaction region [16]; the range of D covered by the distribution scales as $\propto \sqrt{E_k}$. Contributions for different E_k add up to the total distribution. Primarily, E_k varies by ~4.5 eV depending on the vibrational state of the H_2 fragment. In addition, rotational excitation can both increase and decrease E_k, depending on whether it is present in the initial H_3^+ ion or in the H_2 fragment; however, even for considerable rotational excitation the associated shifts in E_k will be small compared to the effect of the vibrational fragment excitation. Neglecting for the moment rotational excitation both in the initial and in the final state, we fitted the observed $P(D)$ by a superposition of projected distributions for various $H_2(v)$ final states, assuming isotropic dissociation and using the relative vibrational state populations as fit parameters. The resulting vibrational distribution [Fig. 1(b)] is found to be wide with a peak around $v = 5$. The good fit at $D > 15$ mm supports the assumption of isotropic dissociation.

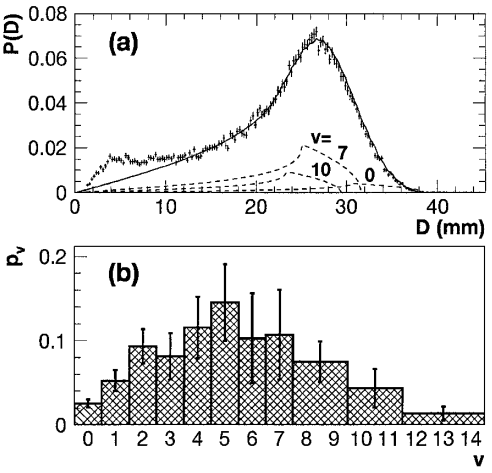

FIG. 1. (a) Projected distance distribution $P(D)$ measured for two-body dissociative recombination. An overall fit using a weighted sum of calculated distributions for the various final vibrational levels v (neglecting rotational excitations) is shown together with the individual contributions for $v = 0, 7$, and 10 (multiplied by 2 for clarity). (b) Relative populations of the final vibrational levels v obtained from the fit (with statistical errors). Rotational excitation leads to an uncertainty of about one level in the v scale.

The vibrational state distribution obtained here provides the first quantitative evidence about product excitation in two-body DR of H_3^+. In comparison with related results for the predissociation of $n = 3$ Rydberg states in H_3 [2], the present fragment state distribution is found to be even wider. Also, peaks around certain excited vibrational levels, as observed for some initial Rydberg states in the H_3 experiment [2], are not observed here.

The projected momenta of the reconstructed three-body events yield information about two aspects: First, the sum R^2 of the squared fragment distances on the imaging detector from the center of mass reflects the total transverse energy of the fragments. Similar to the two-body fragment distance spectra, the end point of the R^2 distribution corresponds to three H fragments arriving in a plane face on at the detector from the most distant interaction point with the maximum energy release E_k. The energy release yielding the observed end point is ~1.3 eV larger than the one corresponding to three H fragments from ground state H_3^+. The internal energies of the atomic H fragments being fixed, the measured excess in E_k indicates internal

excitation of the stored H_3^+ ions; since the CEI measurement showed these ions to be vibrationally cold, the data thus indicate substantial rotational excitation. Assuming H_3^+ ions in the vibrational ground state, but with a rotational temperature of 0.23(3) eV, a good fit to the R^2 end point spectrum is obtained. We consider that the presence of this initial rotational excitation, together with the possibility of rotational excitation in the H_2 fragments, yields an uncertainty of about one level for the vibrational distribution derived from the fit in Fig. 1. In addition, for the given rotational temperature a few percent of the events should have initial energies high enough to reach the final channels $H(n = 2) + H_2(v)$ which open 0.97 eV above the H_3^+ ground state; we therefore tentatively attribute the peak at low D in Fig. 1(a) to events leading to these final states.

The second aspect revealed by the three-body events is the fragmentation geometry, as represented by the shape of the triangle spanned by the momentum vectors of the three H atoms. In general, this triangle is arbitrarily oriented in space, its size is characterized by the energy release E_k, and its shape can be uniquely specified by the coordinates $\eta_1 = (2E_3 - E_2 - E_1)/3E_k$ and $\eta_2 = (E_2 - E_1)/\sqrt{3}\,E_k$ describing the energy sharing between the fragments (where E_i denote the fragment energies in the center of mass frame). In these coordinates (the Dalitz [17] coordinates frequently used in high-energy physics), events from a dissociation process producing uncorrelated momentum vectors would yield a uniform distribution [3]. In our experiment, on the other hand, we only obtain the shape of the fragment momentum triangle as projected onto the detector plane, and hence choose a similar representation using the coordinates $Q_1 = (2R_3^2 - R_2^2 - R_1^2)/3R^2$ and $Q_2 = (R_2^2 - R_1^2)/\sqrt{3}\,R^2$ derived from the transverse fragment distances R_i to the center of mass. The histogram of the measured events [18] over the coordinates Q_1, Q_2 is shown in Fig. 2(a). For comparison, a histogram in Q_1, Q_2 was obtained by simulating the same number of events [Fig. 2(b)], including the detector resolution and efficiency, and assuming uncorrelated momentum vectors in space. Although the two histograms [Figs. 2(a) and 2(b)] look similar, the ratio of the experimental to the random simulated histogram [Fig. 2(c)] reveals distinct differences: linear back-to-back emission of two H atoms from the dissociating H_3 complex [cf. Fig. 2(d)] appears to be enhanced, while equilateral dissociation is observed less often. In addition, among the linear geometries (situated along the circular boundary in the Q_1, Q_2 plot), those where two H atoms go to nearly the same direction occur less often.

Both findings in the first place apply to the projected momenta. However, more detailed conclusions about the 3-H momentum geometries before projection can be drawn under the assumption that the dissociation planes are isotropically oriented in space over a large sample of events. We consider this assumption to hold since the shape of the D distribution for two-body events, as

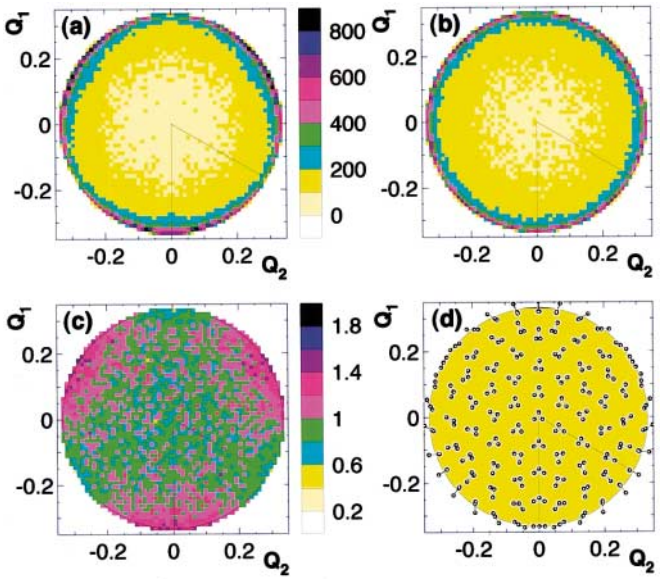

FIG. 2 (color). Distribution of the three-body dissociation events over coordinates Q_1, Q_2 describing the shape of the projected fragment momentum triangle. (a) Measured data ($\sim 7 \times 10^4$ events), symmetrized with respect to exchange of the fragments; (b) simulated data for isotropic uncorrelated dissociation (unsymmetrized); (c) ratio of measured to simulated distribution; (d) shapes of the projected momentum triangle (as seen on the imaging detector) associated with the Q_1, Q_2 coordinates. The 60° sector delimits a symmetry cell of the coordinate plane.

discussed above, is compatible with the one expected for isotropic dissociation. On this basis we have determined the point spread function for given Dalitz coordinates η_1, η_2 in the experimental Q_1, Q_2 plot, using a computer simulation accounting also for experimental details such as the closest distance between two resolved fragment impacts. A Monte Carlo restoration technique [19] is then used to deconvolute the Q_1, Q_2 histogram, yielding a reconstructed Dalitz plot of the 3-H momentum geometries after DR [Fig. 3(a)]. The density distribution in

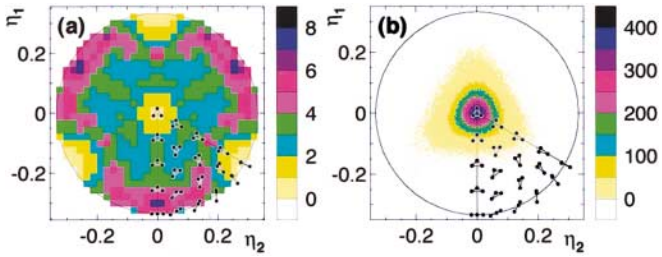

FIG. 3 (color). Yield of 3-H momentum geometries as represented by the Dalitz coordinates η_1, η_2. (a) Distribution for three-body dissociative recombination reconstructed from the measured transverse fragment coordinates (arbitrary normalization); (b) measured distribution for Coulomb explosion of H_3^+ molecules extracted from the storage ring after vibrational relaxation. Shapes of the momentum triangle associated with the η_1, η_2 coordinates are indicated within a symmetry cell.

this plot shows a contrast of about a factor of 3 between nearly linear, approximately symmetric dissociation events and those with equilateral or strongly asymmetric linear momentum geometries. We can compare this distribution directly to the fragmentation geometries found when H_3^+ ions are extracted from the ring and passed through a thin foil, performing Coulomb explosion imaging. Here, a good timing resolution of the imaging detector allows us to measure the fragment energies E_i for each event and to directly construct an η_1, η_2 Dalitz plot [Fig. 3(b)]. The dissociation in this case proceeds via a purely Coulombic interaction and reflects directly the equilateral nuclear conformation of the H_3^+ ion. The striking difference between the two Dalitz plots of Fig. 3 thus displays the strong influence of the H_3 molecular potential surface onto the dynamics of the DR process.

With the plot in Fig. 3(a), experimental data on three-body correlation in the DR of H_3^+ can for the first time be compared against theoretical calculations considering the nuclear motion on the dissociative H_3 potential surfaces. The same surfaces are responsible for the predissociation of H_3 Rydberg states, and wave-packet calculations for such dissociation have been performed [20,21] for the $H + H_2$ and also the 3-H channel. In a two-dimensional calculation [restricted to the isosceles (C_{2v}) geometry] using diabatic potential surfaces, predominance of linear fragmentation was found for the three-body channel [20], while a later calculation [21] without the geometrical restriction, but using adiabatic potential surfaces, found predominance of triangular structures. Our data rather agree with the first calculation [20].

Fragment correlation in the three-body breakup of triatomic hydrogen has recently been measured by Müller *et al.* [3] from single rovibronic Rydberg states of H_3. The Dalitz histograms were found to be highly structured and very sensitive to the initial state symmetry, which was attributed to different coupling mechanisms with the dissociative states. The intermediate states populated by electron capture should in general include many other symmetries and be much shorter lived in comparison to the states of nanosecond lifetimes accessed by Müller *et al.*; therefore, a much less structured Dalitz plot can be expected in our case.

While the predominance of linear momentum geometries in the DR of H_3^+ may at first appear surprising, it might in fact find a plausible explanation in a simple physical picture. Linear dissociation should be favored if two of the H atoms feel a stronger repelling force between them than from the third fragment. After electron capture on H_3^+ (having a singlet ground state), the H atoms in the dissociating H_3 complex find themselves in a superposition of spin states where always two of the atoms have parallel spins. Hence, in three-body dissociation only one pair of H atoms is expected to experience the strongly repelling potential associated with a triplet configuration of the two electron spins, while with respect to the third H atom each atom of this pair would be in a singlet spin configuration, yielding attraction rather than repulsion; forces favoring linear dissociation thus appear plausible. Further theoretical calculations regarding the dissociation in this simple polyatomic system are clearly desirable.

As shown above, our data also yield information about the internal excitation of the H_3^+ beam, produced in a fashion similar to that used in other storage ring experiments. After storage for 3 s, the ion beam appears from recombination fragment imaging to be still strongly rotationally excited, while Coulomb explosion imaging of molecules extracted from the ring confirms the vibrational relaxation to be complete.

This work has been funded in part by the German Federal Minister for Education, Science, Research and Technology (BMBF) under Contract No. 06 HD 854 I and within the framework of the German-Israeli Project Cooperation in Future-Oriented Topics (DIP).

*To whom correspondence should be addressed.
Email address: fndaniel@wicc.weizmann.ac.il

[1] T. N. Kitsopoulos, M. A. Buntine, D. P. Baldwin, R. N. Zare, and D. W. Chandler, Science **260**, 1605 (1993).
[2] U. Müller and P. C. Cosby, J. Chem. Phys. **105**, 3532 (1996).
[3] U. Müller, Th. Eckert, M. Braun, and H. Helm, Phys. Rev. Lett. **83**, 2718 (1999).
[4] D. Azinovic *et al.,* Phys. Rev. A **58**, 1115 (1998).
[5] T. R. Geballe and T. Oka, Nature (London) **384**, 334 (1996).
[6] M. Larsson, Annu. Rev. Phys. Chem. **48**, 151 (1997), and references therein.
[7] B. J. McCall, T. R. Geballe, K. H. Hinkle, and T. Oka, Science **279**, 1910 (1998).
[8] D. Zajfman *et al.,* Phys. Rev. Lett. **75**, 814 (1995).
[9] T. Gougousi, R. Johnsen, and M. F. Golde, Int. J. Mass Spectrom. Ion Process. **149/150**, 131 (1995).
[10] B. J. McCall and T. Oka, Science **287**, 5460 (2000).
[11] A. Suzor-Weiner (private communication).
[12] S. Datz *et al.,* Phys. Rev. Lett. **74**, 896 (1995).
[13] D. Habs *et al.,* Nucl. Instrum. Methods Phys. Res., Sect. B **43**, 390 (1989).
[14] Z. Vager, R. Naaman, and E. P. Kanter, Science **244**, 426 (1989).
[15] R. Wester *et al.,* Nucl. Instrum. Methods Phys. Res., Sect. A **413**, 379 (1998).
[16] Z. Amitay *et al.,* Phys. Rev. A **54**, 4032 (1996).
[17] R. H. Dalitz, Philos. Mag. **44**, 1068 (1953).
[18] In the Dalitz (η_1, η_2) plane and also in the (Q_1, Q_2) plane of the transverse data, events are restricted from momentum conservation to a circle of radius $1/3$.
[19] B. R. Frieden, in *Picture Processing and Digital Filtering,* edited by T. S. Huang (Springer-Verlag, Berlin, 1979), p. 240.
[20] A. E. Orel and K. C. Kulander, J. Chem. Phys. **91**, 6086 (1989).
[21] J. L. Krause, K. C. Kulander, J. C. Light, and A. E. Orel, J. Chem. Phys. **96**, 4283 (1992).